International Immunopharmacology 40 (2016) 400–409

Contents lists available at ScienceDirect

International Immunopharmacology

journal homepage: www.elsevier.com/locate/intimp

Anticancer effect of SZC015 on lung cancer cells through ROS-dependent apoptosis and autophagy induction mechanisms in vitro

Bin Sun [a], Lei Gao [a], Anil Ahsan [a], Peng Chu [a], Yanlin Song [a], Hailong Li [a], Zonghui Zhang [a], Yuan Lin [a], Jinyong Peng [a], Zhicheng Song [b], Shisheng Wang [b,*,1], Zeyao Tang [a,*,1]

[a] Pharmacology Department, Dalian Medical University, 9 West Section, South Road of Lvshun, Dalian, China
[b] College of Pharmaceutical Science and Technology, Dalian University of Technology, Dalian, China

ARTICLE INFO

Article history:
Received 12 May 2016
Received in revised form 31 August 2016
Accepted 24 September 2016
Available online xxxx

Keywords:
SZC015
Apoptosis
Autophagy
Akt/NF-κB signaling
Lung cancer cells

ABSTRACT

Oleanolic acid (OA) and its several derivatives possess various pharmacological activities, such as antitumor and anti-inflammation. In present study, anticancer effect of SZC015, an OA derivative, and its underlying mechanisms were investigated. We demonstrated that cell viability was significantly decreased in SZC015-treated lung cancer cells, but has less cytotoxicity in human bronchial epithelial cell line. Further investigation verified that apoptosis and autophagy induction and G_0/G_1 phase arrest were observed in SZC015-treated H322 cells. Mechanically, the level of Akt, p-Akt, p-IκBα, and total p65, the p-p65 in the cytoplasm and nucleus were suppressed by SZC015 in H322 cells, respectively. Inhibition of p65 nuclear translocation was also confirmed by immunofluorescence staining. In addition, co-treatment with chloroquine, an autophagy inhibitor, significantly inhibited SZC015-induced autophagy and enhanced SZC015-induced apoptotic cell death. Intracellular ROS was increased in a concentration-dependent manner, which could be prevented by N-Acetyl L-Cysteine, an ROS scavenger. Moreover, the level of Akt and procaspase-3 were increased, while the ratio of LC3 II/I was decreased. Taken together, our study demonstrates that the inhibitory effect of SZC015 against H322 cells is mediated by excessive ROS generation that could suppress Akt/NF-κB signaling pathway, which thereby leads to apoptotic and autophagic cell death.

1. Introduction

Lung cancer is the most frequently diagnosed malignancy and the leading cause of the cancer-related death among the world. There are >220,000 cases, which account for approximately 25% of all cancer-related deaths, died each year, and the 5-year survival rate is still <18%, which is lower than the rate for most cancer types [1,2]. Based on the histology, the most prevalent type of lung cancer is non-small-cell lung cancer (NSCLC). The life has been prolonged for the patients with NSCLC due to the application of systemic chemotherapy, especially the postoperative chemotherapy that has been shown to increase the survival rate of lung cancer in many clinical trials [3]. However, since the long-term survival rate of NSCLC patients remains pretty low, there is still urgent to develop novel strategies for NSCLC patients.

Recently, attention has been focused on developing active herbal medicines isolated from natural products, which have been thought to be the important and safe, and some of them are currently evaluated in preclinical and clinical practice [4]. Oleanolic acid (OA, 3β-hydroxyolean-12-en-28-oic acid) is a ubiquitous pentacyclic multifunctional triterpenoid, which can be widely found in several natural plants. The synthetic oleanane triterpenoids are a class of multifunctional compounds that have been used to inhibit cancer progression in a variety of cancer types [2]. CDDO (2-cyano-3, 12-dioxooleana-1,9 (11)-dien-28-oic acid) and its methyl ester (CDDO-Me) are currently found to be efficient for the treatment of leukemia and many solid tumors. Some other derivatives of CDDO such as CDDO-Im (imidazolides), CDDO-MA (methyl amide), and CDDO-EA (ethyl amide) are proved to be effective in killing several cancer types [5,6]. Therefore, novel derivatives of OA need to be synthesized and investigated for their anticancer functions.

In this present study, we aimed to examine the anticancer effect of SZC015, a new novel derivative of oleanolic acid synthesized firstly by us, on human lung cancer cells, and to elucidate the most probable molecular mechanisms involved in its action. SZC015 effectively decreased the cell viability of H322, H1299 and A549 cancer cell lines and has less cytotoxicity in HBE cell line. We also confirmed that apoptotic and autophagy induction and Akt/NF-κB signaling inhibition were mediated by the generation of ROS in H322 cells. In this respect, we firstly report

* Corresponding authors.
E-mail addresses: wangss@dlut.edu.cn (S. Wang), tangzeyao@aliyun.com (Z. Tang).
[1] Equal correspondence contributors.

http://dx.doi.org/10.1016/j.intimp.2016.09.026
1567-5769/

that the potential anticancer effect and mechanisms of SZC015 on human lung cancer cell line H322.

2. Materials and methods

2.1. Chemicals

Oleanolic acid (OA), SZC009, SZC014, SZC015 were friendly provided by Professor Shisheng Wang from Dalian University of Technology. Roswell Park Memorial Institute 1640 (RPMI1640), fetal bovine serum, and 3-[4,5-dimethylthiazolyl-2] 2,5-diphenyl-tetrazolium bromide (MTT) were purchased from Gibco (Gaithersburg, MD, USA). N-Acetyl-L-Cysteine (NAC) was obtained from Sigma-Aldrich (St Louis, MO, USA). The 6-carboxy-2′,7′-dichlorodihydrofluorescein diacetate (DCFH-DA) and 4′,6-diamidino-2-phenylindole (DAPI) were purchased from the Beyotime Institute of Biotechnology (Haimen, Jiangsu, China). The Annexin V-FITC Apoptosis Detection Kit and Propidium Iodide were purchased from the Nanjing Jiancheng Bioengineering Institute (Haimen, Jiangsu, China). The primary antibodies against Akt, p-Akt, p65, p-p65, p-IκBα, procaspase-9, procaspase-3, Bax, Bcl-2, LC3B, β-actin, Histone *H*3 and the second antibody goat anti-rabbit IgG-horseradish peroxidase were purchased from the Proteintech (Chicago, IL, USA).

2.2. 3-Oxo-olean-12-en-28-oic acid (OA)

OA 2.0 g (4.4 mmol) was dissolved in 100 ml mixed solvent of dichloromethane and acetone (volume ratio of 1:1). The solution was cooled to 0 °C, and 2.0 ml Jones reagent was added dropwise within 30 min. The reaction mixture was stirred for 30 min and 2 ml isopropanol was added. After 10 min, the mixture was filtered, and the filtrate was evaporated under reduced pressure to yield a solid residue, which was dissolved in 50 ml ethyl acetate, then washed with saturated brine (50 ml × 3). The organic phase was dried with anhydrous sodium sulfate and concentrated in vacuo. The crude product was purified by silica gel column chromatography eluting with petroleum ether/ethyl acetate (20:1, V: V) to afford 3-oxo-OA as a white solid (1.97 g, 98.2% yield). m p. 181–182 °C. Positive ESI-TOF-MS: *m/z* 499.2864 $(M + 2Na\text{-}H)^+$. ^1H NMR ($CDCl_3$, 400 MHz): 0.81, 0.91, 0.93, 1.03, 1.05, 1.08, 1.15 (each s, 3H, 7 × CH3), 5.30 (1H, t, $J = 3.3$ Hz, H-12), 2.84 (1H, dd, $J = 13.6$, 3.8 Hz, H-18), 2.33–2.55 (2H, m, H-2).

2.3. 2-Morpholinomethyl-3-oxo-olean-12-en-28-oic acid (SZC015)

Morpholine hydrochloride 1.23 g (10.0 mmol), $SnCl_2$ 0.38 g (2.0 mmol) and paraformaldehyde 0.3 g were added to a solution of 3-oxo-OA (0.91 g, 2.0 mmol) in 40 ml ethanol. The reaction mixture was heated at reflux for 20 h and then filtrated. The filtrate was concentrated to dryness under reduced pressure. The residue was dissolved in 200 ml ethyl acetate, then washed with saturated brine (50 ml × 3). The organic layer was dried with anhydrous sodium sulfate and concentrated in vacuo. The crude product was purified by silica gel column chromatography eluting with chloroform/ethanol/water (15:1:0.1, V:V:V) to give compound SZC015 as a pale yellow solid (0.17 g, 15.3% yield). mp 162–164 °C. MS (API-ES Negative)*m/z*:588.5 $(M + Cl)^-$;(API-ES Positive)m/z 554.5$(M + H)^+$. ^1H NMR ($CDCl_3$, 400 MHz), 0.83, 0.90, 0.93, 1.07, 1.10, 1.11, 1.22 (each s, 3H, 7 × CH_3), 2.59 (t, 4H, $N(\underline{CH_2}CH_2)_2O$), 2.85 (dd, 1H, $J = 3.4$, 13.0 Hz, H-18), 3.77 (brs, 4H, $N(CH_2\underline{CH_2})_2O$), 5.29 (brs, 1H, $J = 3.3$ Hz, H-12). ^{13}C NMR (100 MHz, $CDCl_3$), δ: 207.4, 183.0, 143.7, 122.2, 66.4, 58.2, 54.1, 53.4, 52.8, 48.5, 47.9, 47.1, 47.0, 46.6, 45.4, 41.9, 41.9, 39.5, 39.1, 38.6, 36.7, 33.9, 32.5, 30.7, 29.7, 28.2, 25.8, 25.8, 25.4, 23.7, 20.2, 18.0, 17.3. The derivatives were dissolved in DMSO and stored at 4 °C.

2.4. Cell culture

The human non-small-cell lung cancer cell lines H322, H1299, A549 and the human bronchial epithelial cell line HBE were kindly provided by Dalian Medical University Cancer Center. All cell lines were cultured in RPMI 1640 medium containing 10% fetal bovine serum, penicillin (100 units/ml) and streptomycin (100 μg/ml) in 95% humidified air atmosphere with 5% CO_2 at 37 °C.

2.5. MTT assay

Cell viability was estimated by MTT assay as previously introduced [7]. Briefly, cells were seeded in 96-well plates at a density of (1×10^5 cells/ml) and then incubated at 37 °C for 24 h. After treatment with different concentrations of OA, SZC009, SZC014 and SZC015, 15 μl MTT stock solution (5 mg/ml) was added to each well. After 4 h of incubation, 100 μl SDS-isobutanol-HCl solution (10% SDS, 5% isobutanol and 12 mM HCl) was added to dissolve the formazan crystals and the plates were further incubated at 37 °C for overnight. The light absorption was recorded at a wavelength of 570 nm with an Enzyme mark instrument (Thermo-354, USA).

2.6. DAPI staining

To determine the inhibition effect of SZC015, the 4′,6-diamidino-2-phenylindole (DAPI) assay was performed. Briefly, H322 cells (2×10^5 cells/ml) were cultured in 6-well plate, incubated at 37 °C for 24 h. After an exposure to SZC015 for 24 h, cells were washed with PBS and fixed with 10% formaldehyde for 10 min. Cells were subsequently stained with DAPI (1 μg/ml) for 8 min in the darkness at room temperature. Then washed with PBS for three times. At last, the pictures were taken by using a fluorescence microscope (Nikon, Japan).

2.7. Transmission electron microscopy

H322 cells (2×10^5 cells/ml) were plated into a 6-well plate and further incubated at 37 °C for 24 h. After treatment with SZC015 (20 μmol/l) for 24 h, cells were washed, collected, and prefixed in 2.5% glutaraldehyde overnight at 4 °C. Cells were then post fixed in osmium tetroxide for 30 min, dehydrated in a 10% graded series of 50%–100% ethanol, and embedded in the Epon 812 resin. The ultrathin sections were cut and stained. Finally, the ultrathin sections were stained and imaged using a transmission electron microscope (JEM-2000EX; JEOL Co; Japan).

2.8. Cell apoptosis analysis

To determine whether apoptosis involves in the inhibition effect of SZC015 on cell viability in H322 cells, the Annexin V-FITC Apoptosis Detection kit was used according to the manufacturer's instructions. Briefly, H322 cells were seeded in 6-well plates and further cultured at 37 °C for 24 h. Then cells were treated with different concentrations of SZC015 for 24 h. H322 cells were washed, harvested, and collected. Finally, the samples were stained with 5 μl of Annexin-V FITC and propidium iodide for 30 min in the dark at room temperature. These samples were then analyzed by flow cytometry immediately (BD FACSAria II; BD Co; America).

2.9. Propidium iodide staining

To determine whether cell cycle arrest involves in the inhibition effect of SZC015 on cell viability in H322 cells. Cells were plated in 6-well plates, incubated at 37 °C for 24 h then cells were treated with different concentrations of SZC015 for 24 h, subsequently collected, and fixed in 70% cold ethanol overnight at 4 °C. The samples were resuspended with the cell cycle analysis solution that contains 50 mg/ml PI and 1 mg/ml RNAse in 1 ml of sodium citrate buffer, and then incubated in

the dark for 30 min. The distribution of cell cycle was determined by flow cytometry (BD FACSAria II; BD Co; America).

2.10. Intracellular reactive oxygen species (ROS) level detection

The production of intracellular ROS was measured by flow cytometry using the Reactive Oxygen Species Assay Kit according to the manufacturer's instructions. Briefly, H322 cells were cultured in 6-well plates, incubated at 37 °C for 24 h then cells were treated with different concentrations of SZC015 for 24 h. At the end of time, cells were washed and collected by PBS for three times. After that, cells were suspended with serum-free medium containing 10 μM DCFH-DA at dark for 30 min. After washing with serum-free medium for three times, cells were analyzed with flow cytometry (BD FACSAria II; BD Co; America).

2.11. Immunofluorescence staining for NF-κB p65 localization

Immunofluorescence staining was performed to determine the effect of SZC015 on the nuclear translocation of p65 in H322 cells. Cells were plated and cultured in chamber slides. After treatment with different concentrations of SZC015 for 24 h, cells were washed with PBS for one time and fixed with 4% paraformaldehyde for 15 min at room temperature. Samples were permeabilized with 0.4% TritonX-100 for 10 min, and then blocked with 2% bovine serum albumin (BSA) in PBS for 1 h at 37 °C. Primary antibody against p65 in the 1% blocking solution was added into the wells and the plates were further cultured for overnight at 4 °C. Following washing with PBS of samples, fluorescein-conjugated secondary antibody was added in 1% blocking solutions and incubated for 1 h. Finally, the samples were stained with DAPI (1 μg/ml) for 10 min to stain the cell nuclei. The samples were examined by using a fluorescence microscope (Labophot 2; Nikon, Tokyo, Japan).

2.12. Western blot analysis

The H322 cells (2×10^5 cells/ml) were plated in 6-well plates and treated with SZC015 for 24 h. The cytoplasmic and nuclear protein samples were extracted with cell lysis kits. Total protein was denatured by dissolving in 5× sample buffer and boiled for 5 min at 100 °C. Samples (~20 μg) were loaded onto the SDS-PAGE gel (10–15%), separated by gel electrophoresis, and then transferred onto PVDF membranes (Millipore, Bedford, MA, USA). After blocking with 5% skimmed milk in TBS containing 0.05% Tween 20 (TTBS) at room temperature for 2 h, the membranes were incubated with primary antibody (1:1000 dilution) for overnight at 4 °C. Thereafter, the blots were washed three times with TTBS, then the membranes were incubated with horseradish peroxidase-conjugated secondary antibody (1:1000 dilution) for 1 h at 4 °C. After washing three times, the membranes were detected by using an enhanced chemiluminescence method and photographed by Bio-Spectrum Gel Imaging System. The data were adjusted to β-actin expression [integral optical density value (IOD) of the target protein versus IOD of β-actin] to eliminate the variations.

2.13. Statistical analysis

All the data were performed using Graph Pad Prism 6 (Graph Pad Software, Inc., San Diego, CA) and expressed as mean ± SD from at least three independent experiments. One-way ANOVA test was used to analyze statistical differences between groups. p value < 0.05 was regarded as statistically significant.

3. Results

3.1. SZC015 inhibits cell viability in lung cancer cells

We initially examine the effect of OA, SZC009, SZC014 and SZC015 on cell viability in H322, H1299, and A549 cell lines by MTT assay. The data showed that SZC015 expressed more cytotoxicity than other drugs, and SZC015 inhibited human non-small-cell lung cancer cell lines H322, H1299, and A549 in a time and concentration dependent manner as shown in Fig. 1. The half maximal inhibitory concentration value (IC_{50}) values of SZC015 for 24 h of H322, H1299, and A549 cells were 22.28, 50.84 and 67.62 μmol/l respectively. These records demonstrated that the SZC015 exhibited potent antitumor activity and H322 cell line showed more sensitive to the agent. Therefore, H322 was selected to make a further exploration due to its low IC_{50} value after 24 h treatment. As shown in Fig. 2, significantly more HBE cells survived as compared with H322 cell line, indicating that SZC015 showed selective cell viability inhibition effect in kill cancer cells versus normal cells.

3.2. Apoptosis induction effect of SZC015 in H322 cells

The induction of apoptosis was evaluated firstly by microscopic observation, revealed the morphological changes of apoptosis, including cell shrinkage and fragmentation, after treatment with SZC015 as shown in Fig. 3A. DAPI staining is a morphological assessment, was performed to further evaluate apoptosis. DAPI fluorescent staining treated with H322 cells and there were certain changes in apoptotic cells, bright blue light was observed (Fig. 3B). Furthermore, to confirm the apoptosis induction effect of SZC015, we next performed Annexin V-FITC and PI double staining analyzed by flow cytometry. Fig. 3C showed that SZC015 increased the percentage of both early apoptotic cells and late apoptotic cells in a concentration-dependent manner. SZC015 treatment significantly increased the total apoptosis from 7.58% to 21.93% at 0 and 30 μM concentrations respectively. The ultrastructure was observed by transmission electron microscopy (TEM). The normal cells possessed the typical and regular shapes, while a series of apoptotic changes appeared, including loss of microvilli, nucleus chromatin condensation and marginalization, narrowing of nuclei, and an abundant of vacuoles, after treatment with SZC015 as shown in Fig. 3D. To test whether caspases are related to SZC015-induced apoptosis, we next evacuated the level of procaspase-3 and procaspase-9 of SZC015-treated H322 cells by Western blot. Fig. 3E clearly showed that both procaspase-3 and procaspase-9 were suppressed by SZC015 in a concentration-dependent manner and the level of procaspase-3 in Fig. 3G has also been shown the OA pro-apoptotic capacity against H322 cells. We also investigated whether SZC015-induced apoptosis was related with the alterations in the expression of anti-apoptotic protein Bcl-2 and pro-apoptotic protein Bax of SZC015-treated H322 cells as shown in Fig. 3F. We found that a significant increase in Bax/Bcl-2 ratio after treatment with SZC015 was observed. These results suggest that induction of caspases and increase in the Bax/Bcl-2 ratio may be a possible mechanism in SZC015-induced apoptosis.

3.3. SZC015 induces cell cycle arrest

Cell cycle arrest is previously proved to be an important mechanism to inhibit cancer cells [8]. Flow cytometry was performed to investigate the cell cycle distribution in the SZC015-treated H322 cells. As shown in Fig. 4, SZC015 could decrease percentage of the S-phase cells from 45.94% to 32.14%, whereas the percentage of G_2-phase cells was changed unapparently. Nevertheless, the percentage of cells was significantly increased by SZC015 at G1-phase from 48.66% to 59.86%. These results suggested that SZC015-induced cell viability inhibition is associated with the cell cycle arrest at G_1 phase.

3.4. SZC015 induces autophagy in H322 cells

Autophagy is a fundamental biological process in mammalian cells, which can be detected by many ways including TEM and LC3 level by Western blot [9]. Accumulation of auto phagosomes inside SZC015-treated H322 cells were obviously confirmed by TEM, as compared with control group (Fig. 5A). Consistent with previous study [10], we

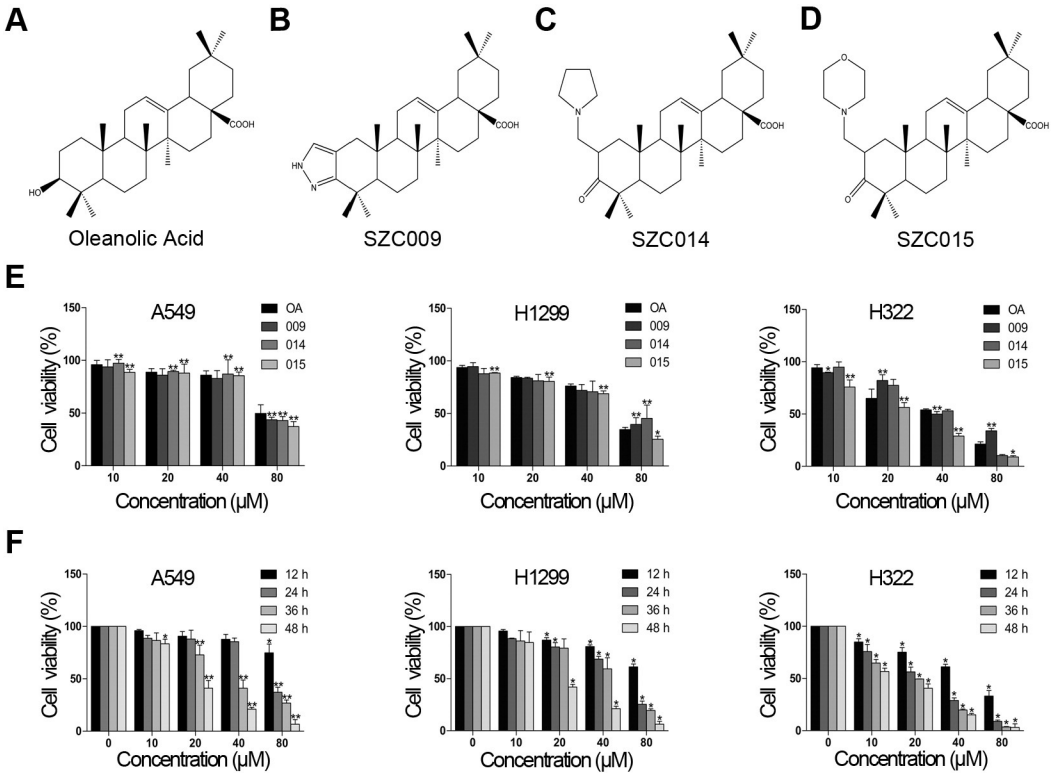

Fig. 1. Growth inhibition by SZC015 in lung cancer cells. **A.** The chemical structure of OA. **B.** The chemical structure of SZC009. **C.** The chemical structure of SZC014. **D**. The chemical structure of SZC015. **E.** The inhibitory effect of OA, SZC009. SZC014, SZC015 on A549, H1299, and H322 cell lines respectively. Cells were treated with different concentrations ranging from 10 to 80 μM for 24 h and cell viability was analyzed by the MTT assay. The data are shown as mean ± SD of three independent experiments. *Significantly different from OA group, $^{**}p < 0.01$, $^{*}p < 0.05$. **F.** The inhibitory effect of SZC015 on cell viability in A549, H1299 and H322 cell lines respectively. Cells were treated with SZC015 (10, 20, 40, and 80 μM) for 12, 24, 36, 48 h and then cell viability was assessed by the MTT assay. The data are expressed as mean ± SD from three independent experiments. *Significantly different from control, $^{**}p < 0.01$, $^{*}p < 0.05$.

verified that OA could also initiate autophagy in H322 cells, and moreover, SZC015 showed a stronger autophagic induction ability than that of OA via calculating the ratio of LC3II/I (Fig. 5B). These data suggested that SZC015 could induce autophagy in H322 cells.

3.5. AKT/NF-κB signaling pathway is an effective target of SZC015 in H322 cells

Chemotherapeutic agents could kill cancer cells via suppressing the Akt signaling pathway, and thus induce cancer cell apoptosis [11]. As shown in Fig. 6A, the activities of both Akt and p-Akt were significantly suppressed by SZC015 in a concentration- dependent manner suggesting that Akt, as an upstream molecule, might be an effective target for SZC015 in H322 cells. NF-κB pathway is a close downstream pathway of Akt and also is involved in regulating cancer cell survival and death. Therefore, we evaluated the level of many NF-κB signaling-related proteins including p-IκBα, p65, and p-p65. Interestingly, both p-IκBα and p65 were downregulated by SZC015 in H322 cells. Then we examined the level of p-p65 in both cytoplasm and nucleus, both of p-p65 in the cytoplasm and nucleus were significantly decreased by SZC015

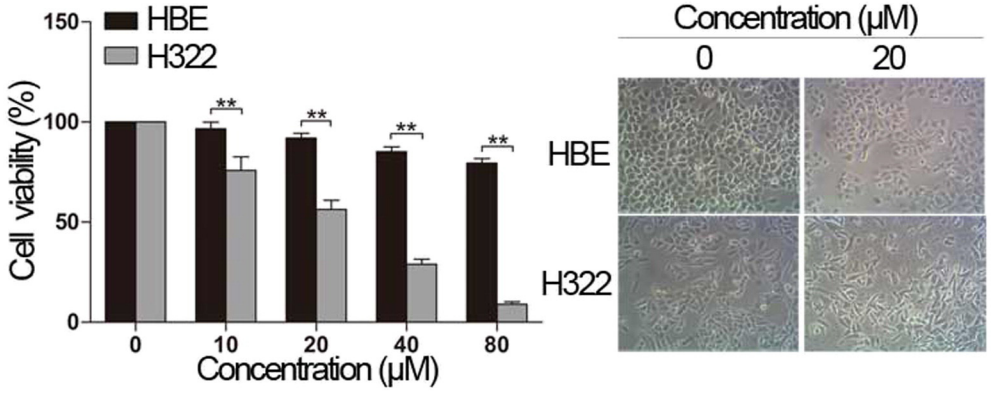

Fig. 2. The selective inhibitory effect of SZC015 on cell viability in HBE and H322 cell lines. Cells were treated with SZC015 (10, 20, 40, and 80 μM) for 24 h, and cell viability was analyzed by the MTT assay. The data are shown as mean ± SD of three independent experiments. *Significantly different from HBE cell lines, $^{**}p < 0.01$, $^{*}p < 0.05$ and the morphology observations were recorded by an inverted phase contrast microscopy.

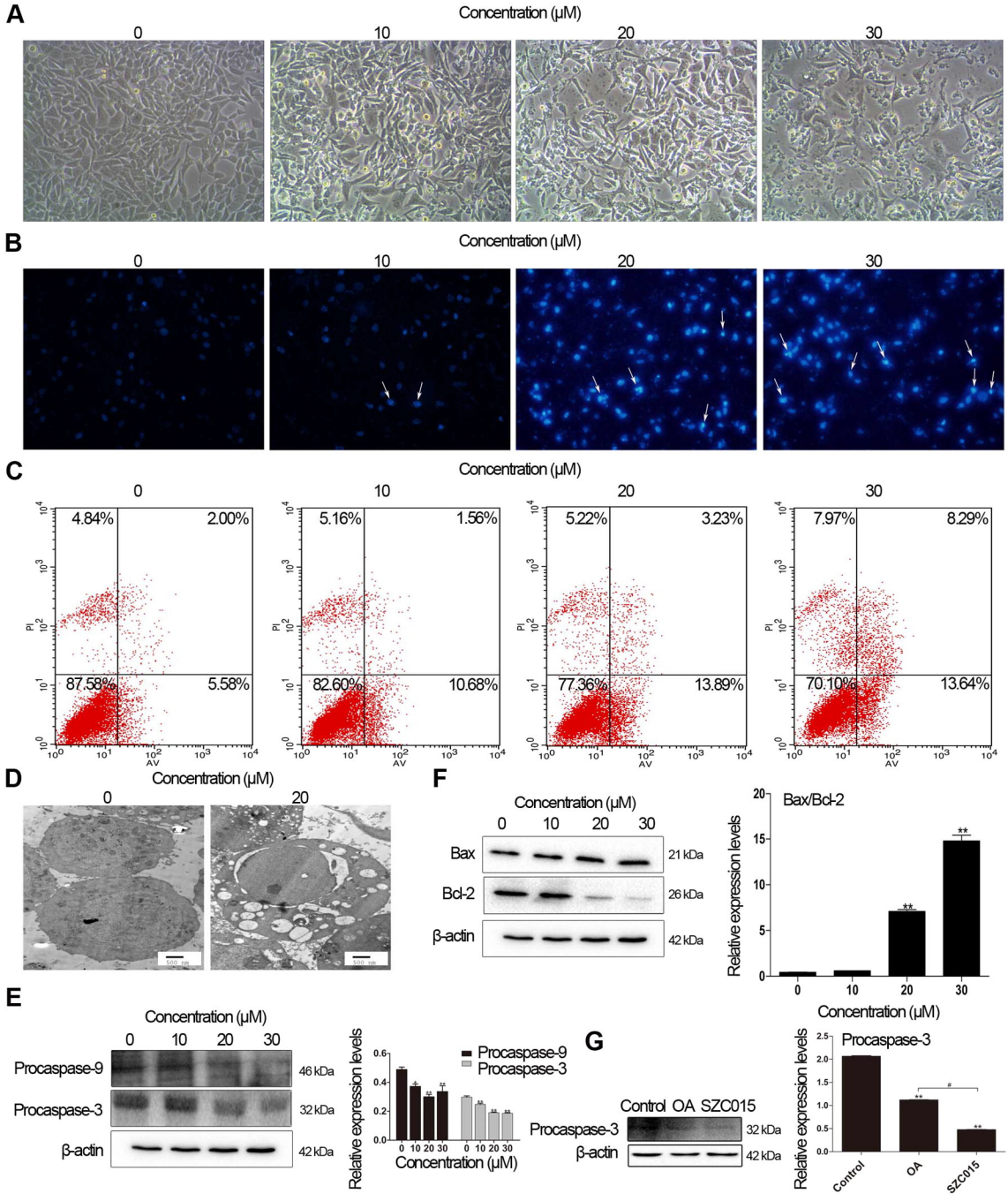

Fig. 3. Induction of apoptosis by SZC015 in H322 cells. **A.** Inverted contrast phase microscopy showed morphology changes of H322 cells treated with SZC015 (10, 20, and 30 μM) for 24 h. **B.** Nuclear condensation and fragmentation are detected by DAPI staining. Bright blue regions indicated nuclear condensation in H322 cells. **C.** Flow cytometry analysis of apoptosis in H322 cells treated with SZC015 at concentrations of 10, 20, and 30 μM for 24 h, samples were then stained with Annexin-V FITC and PI, and analyzed by flow cytometry. **D.** Transmission electron microscopy revealed the occurrence of apoptosis in H322 cells after treatment with 20 μM SZC015 for 24 h. **E.** The expression of procaspase-9 and procaspase-3 protein were determined by Western blotting. The data are shown as mean ± SD of three independent experiments. *Significantly different from control, $^{**}p < 0.01$, $^{*}p < 0.05$. **F.** Western blot analysis for the effect of SZC015 on Bax and Bcl-2. The data are shown as mean ± SD of three independent experiments. *Significantly different from control, $^{**}p < 0.01$, $^{*}p < 0.05$. **G.** The effect of OA and SZC015 on apoptosis in H322 cells. After treatment with OA (20 μM) and SZC015 (20 μM) for 24 h, Western blot analysis of procaspase-3 was evaluated of H322 cells. The data are shown as mean ± SD of three independent experiments. *Significantly different from control, $^{**}p < 0.01$, $^{*}p < 0.05$ and # significantly different from OA group, $\#p < 0.05$. (For interpretation of the references to colour in this figure legend, the reader is referred to the web version of this article.)

(Fig. 6B). To confirm these findings, immunofluorescence analysis detecting p65 inside H322 cells was carried out. As we expected, a constitutive presence of p65 in nucleus of control group was observed, however, p65 was obviously accumulated in cytoplasm, and its expression in nucleus was clearly inhibited after treatment with SZC015 (Fig. 6C). These results indicate that SZC015 can inhibit the Akt/NF-κB signaling pathway.

3.6. SZC015-induced autophagy inhibits cell viability and apoptosis in H322 cells

To determine the role of autophagy induced by SZC015, chloroquine (CQ), an autophagy inhibitor, was used to inhibit autophagy at a later stage. As shown in Fig. 7A, pre-treatment with CQ could prevent H322 cells from death, as compared with the SZC015-only treated the cells,

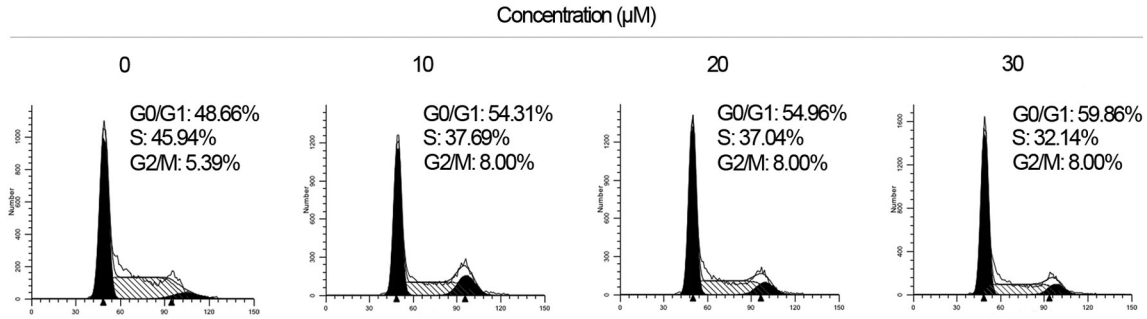

Fig. 4. Flow cytometry analysis of the cell cycle distribution of SZC015-treated H322 cells. Cells were treated with different concentrations of SZC015 (10, 20, and 30 μM) for 24 h.

leading to an untypical morphology change. Pre-treatment with CQ increased the ratio of LC3 II/I (Fig. 7B) suggesting that autophagy induced by SZC015 was inhibited by CQ. Furthermore, to determine the relationship between autophagy and apoptosis induced by SZC015, we next evaluated level of procaspase-3 after pre-treatment with CQ. Fig. 7B clearly showed pre-treatment with CQ dramatically decreased expression of procaspase-3, as compared with SZC015 group only. These data suggest that SZC015-induced autophagy not only prevent cells from SZC015-induced cell death, but also inhibit apoptosis triggered by SZC015 in H322 cells.

3.7. Excessive ROS generation is required for SZC015-induced apoptosis, autophagy, and Akt inhibition

An increasing ratio of Bax/Bcl-2 was observed after treatment with SZC015 (Fig. 3F) suggesting that mitochondrial dysfunction might be caused by SZC015. Mitochondrial dysfunction can result in the increase of ROS generation which in turn will induce cancer cell apoptosis via a mitochondrial stress pathway. Excessive ROS generation was induced by SZC015 in H322 cells. NAC is an antioxidant ROS scavenger that was utilized to clean up ROS [12]. As shown in Fig. 8B, pre-treatment with NAC could prevent excessive ROS generation and prevent apoptosis induced by SZC015. To examine the role of ROS in SZC015-induced apoptosis, autophagy, and Akt inhibition, Western blot analysis was carried out. As shown in Fig. 8C, pre-treatment with NAC not only prevent the cells death but also increase level of procaspase-3 and Akt in SZC015-treated H322 cells. Moreover, pretreatment with NAC decreased the ratio of LC3II/I in SZC015-treated H322 cells. Taken together, excessive ROS generation is an important upstream event of SZC015-induced apoptosis, autophagy, and Akt inhibition.

4. Discussion

Our present study showed that SZC015, a novel derivative of OA, effectively inhibited the proliferation of non-small-cell lung cancer cell

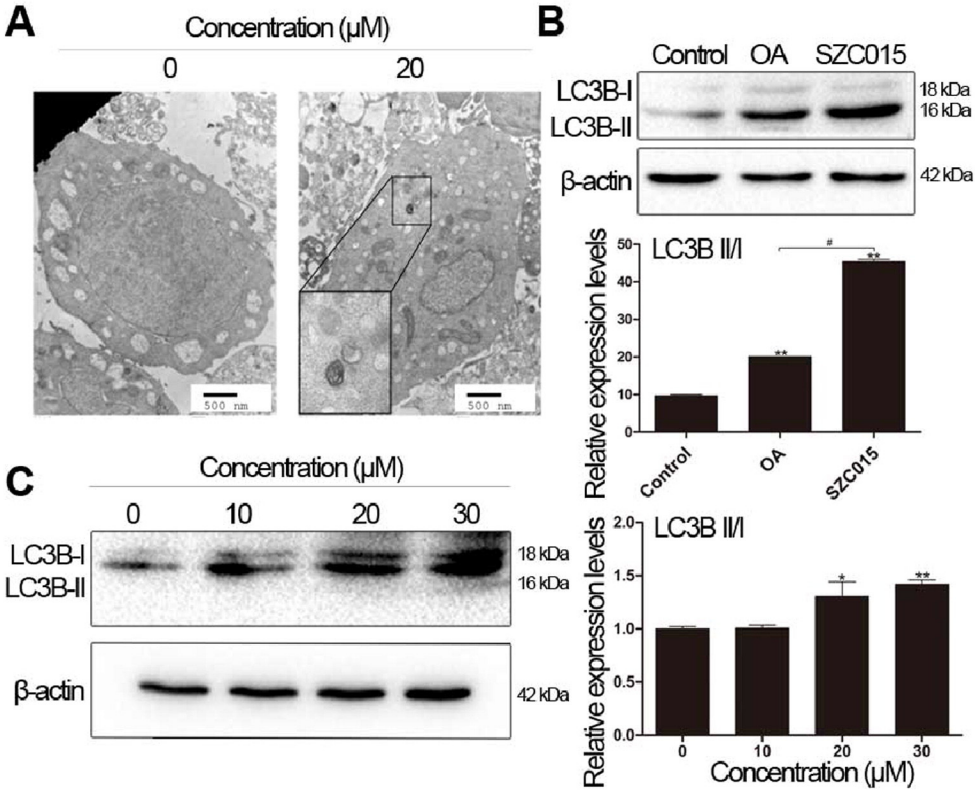

Fig. 5. Autophagy induction effect of SZC015 in H322 cells. **A.** Transmission electron microscopy showed the autophagy existence induced by SZC015 in H322 cells after treatment with 20 μM SZC015 for 24 h. **B.** Western blot analysis of LC3 was evaluated after treatment with SZC015 (20 μM) for 24 h. The data are revealed as mean ± SD of three independent experiments. *Significantly different from control, **$p < 0.01$, *$p < 0.05$ and # significantly different from OA group, #$p < 0.05$. **C.** Western blot analysis was also performed to determine the expression of autophagy-related protein LC3B after 20 μM SZC015 treatment for 24 h in H322 cells. The data are expressed as mean ± SD of three independent experiments. *Significantly different from control, **$p < 0.01$, *$p < 0.05$.

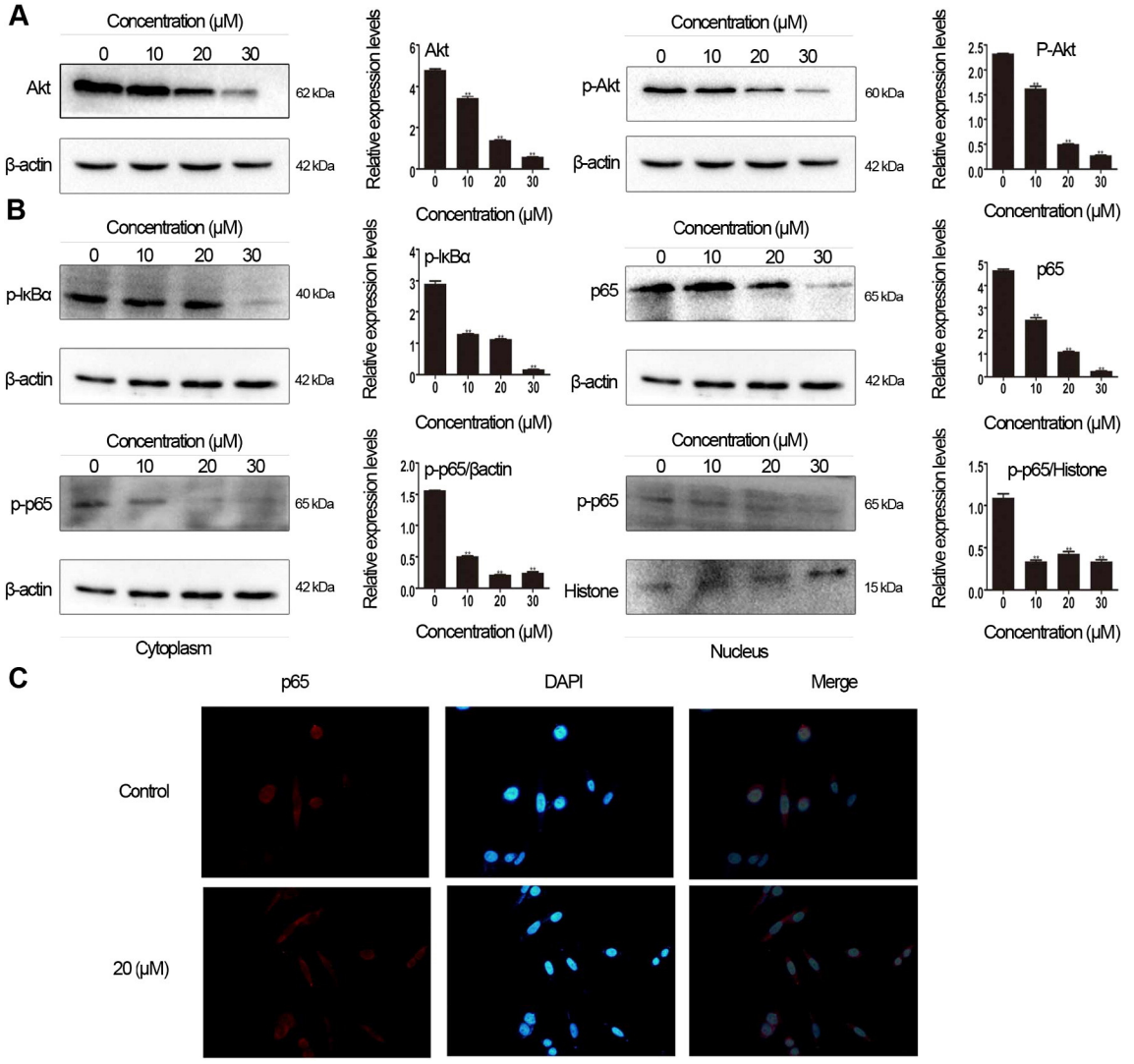

Fig. 6. Inhibitory effect of SZC015 on the Akt/NF-κB pathway. **A.** Western blot analysis of Akt and p-Akt in response to SZC015 treatment in H322 cells. Treatment of H322 cells with SZC015 (10, 20, and 30 μM) for 24 h resulted in suppression of both Akt and p-Akt. The data are shown as mean ± SD of three independent experiments. *Significantly different from control, $^{**}p < 0.01$, $^{*}p < 0.05$. **B.** Western blot analysis of several NF-κB pathway related proteins, containing p-IκBα, total p65 and p-p65 in both cytoplasm and nucleus. H322 cells were treated with SZC015 (10, 20, and 30 μM) for 24 h caused in the changes of these proteins expression. The data are shown as mean ± SD of three independent experiments. *Significantly different from control, $^{**}p < 0.01$, $^{*}p < 0.05$. **C.** Immunofluorescence staining analysis of p65 localization in H322 cells treated with SZC015 (20 μM) for 24 h were labeled for p65 (*red*), and nuclei were stained with DAPI (*blue*). (For interpretation of the references to colour in this figure legend, the reader is referred to the web version of this article.)

lines, especially H322 cell line. Interestingly, OA could induce both apoptosis and autophagy in H322 cell line. Systematically, the generation of intracellular ROS was excessively increased by SZC015 that was demonstrated to be the upstream event among these pharmacological effects. Moreover, our findings also indicated that excessive ROS could suppress the Akt/NF-κB pathway that was a major signaling to inhibit apoptosis and autophagy. Furthermore, our results displayed that SZC015-induced autophagy not only could increase cell viability, but also inhibit apoptosis induced by SZC015.

Apoptosis is also known as programmed cell death is a fundamental process and is essential for the homeostasis of multicellular organisms [13,14]. Previous publications have demonstrated that OA may be a potent anticancer candidate for several cancer types, as evidenced by its proliferation inhibition effect [15,16]. Our results confirmed that SZC015 could trigger the intrinsic apoptosis in H322 cells, and especially possessed a more obvious inhibition effect on cell viability and apoptosis induction effect against H322 cells, as compared with OA. It has been reported that there are two identified pathways of apoptosis: (1) the extrinsic pathway that is initiated by ligand-induced activation of death receptors; (2) the intrinsic pathway that is triggered by many stress signal [17]. Recently, several investigations about derivatives of OA have demonstrated that different modifications of OA can lead to intrinsic apoptosis in many cancer types [18,19]. Remarkably, our results indicated that SZC015 was also an inducer of intrinsic apoptosis in H322 cells. Mechanistically, we evaluated the level of some intrinsic apoptosis-related proteins named procaspase-9, procaspase-3, Bcl-2, and Bax. As expected, SZC015 could significantly decrease the ratio of Bcl-2/Bax (Fig. 3F), which is a key index of intrinsic apoptosis in response to several stimulations, indicating that the mitochondria might be severely damaged by SZC015 [20]. In addition, two essential intrinsic apoptosis proteins, the procaspase-9 and procaspase-3 [21], were also suppressed by SZC015 in a concentration-dependent manner (Fig. 3E). Several studies implied that mitochondria are the major site that produces ROS which may lead to apoptosis subsequently [22], and inhibition of apoptosis by Bcl-2 is associated with protection against ROS [23]. Our results confirmed that excessive ROS could be generated by

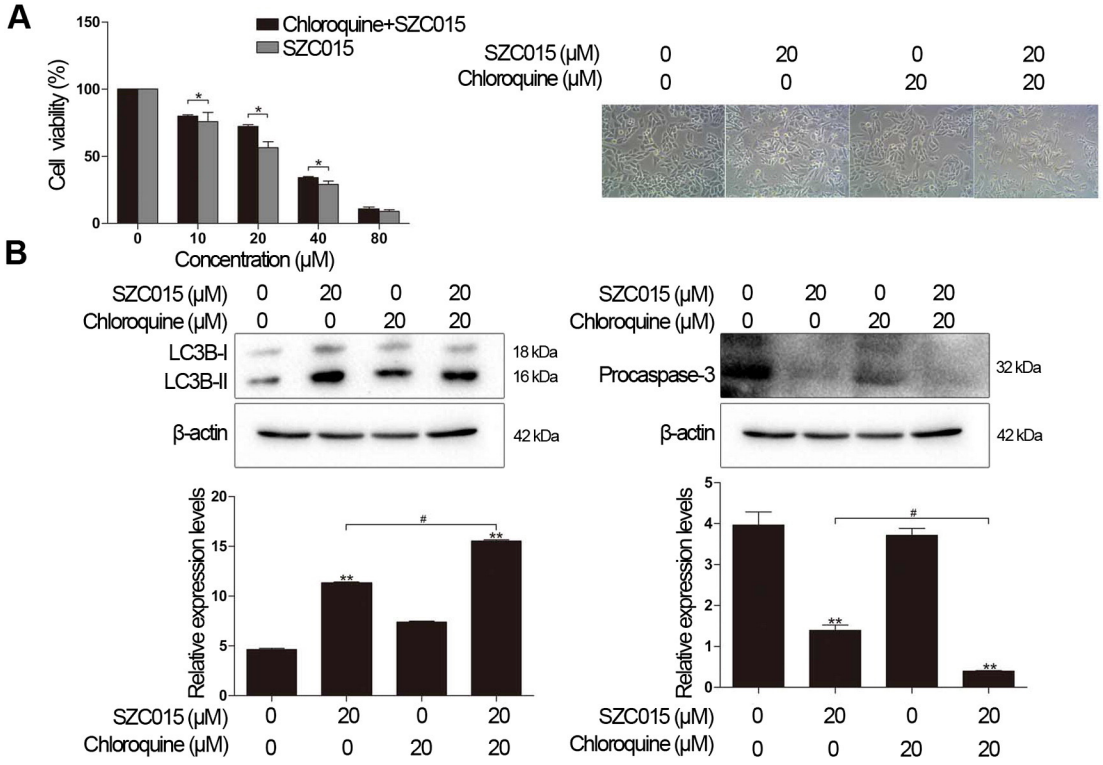

Fig. 7. Effect of the autophagy on the apoptosis in SZC015-treated H322 cells. **A.** Pretreatment with chloroquine (CQ) prevented cells from SZC015-induced inhibition of cell viability. H322 cells were pretreated with CQ (20 μM) for 3 h and then treated with various concentrations of SZC015 (10, 20, 40, and 80 μM) for 24 h. The cell viability was analyzed by MTT assay, and the morphology observations were recorded by an inverted phase contrast microscopy. **B.** Western blot analysis of the expression of LC3 and procaspase-3. H322 cells were pretreated with CQ (20 μM) for 3 h and then 20 μM SZC015 was treated with cells for further 24 h. The data are shown as mean ± SD of three independent experiments. *Significantly different from control, $^{**}p < 0.01$, $^{*}p < 0.05$ and # significantly different from only SZC015 group, $\#p < 0.05$.

SZC015 in H322 cells (Fig. 8A) and ROS was also a dangerous regulator of apoptosis induced by SZC015 (Fig. 8B) suggesting that ROS might be a critical molecule in regulating apoptosis in lung cancer cells.

The NF-kB pathway is very important in modulating several biological process, including cell proliferation, tumorigenesis, and especially the inflammation [24]. Since the activation of PI3K/Akt signaling, the upstream regulator of NF-kB, occurs in >90% of NSCLC patients, it has become an important target for anticancer drugs [11]. Similar to previous studies, the Akt and its active form p-Akt were significantly suppressed by SZC015 in a concentration-dependent manner (Fig. 6A), suggesting that the Akt signaling might be an effective anticancer target of NSCLC by SZC015. In recent publications, several plant-derived compounds are considered to be highly effective in suppressing the Akt pathway and thus lead to cancer cell death in vitro via ROS-dependent mechanism [25]. Excessive ROS generation induced by SZC015 could be effectively blocked by NAC (Fig. 8B). Dramatically, our data displayed that Akt was significantly increased after blocking ROS generation by NAC (Fig. 8B), which in turn could rescue survival rate of cancer cells, indicating that ROS is an upstream modulator of Akt. while NF-κB pathway is considered to be a very important downstream signaling that connects with Akt pathway, and targeting Akt/NF-κB signaling is an effective way for cancer therapy [12,26].

Besides the fact that suppression of NF-κB pathway will trigger apoptosis [27], it has dual roles in modulating autophagy process [28]. NF-κB dimers are usually located in cytoplasm in an inactive form due to its connection with IκBα, an inhibitory protein [29]. In response to many stimulations, IκB kinase (IKK) then is activated and leads to IκBα phosphorylation, ubiquitination, and degradation by proteasomes [30]. Free NF-κB dimers will translocated into nucleus where it will modulate gene expression [31]. Two IκBα-associated ways have been proved to inhibit NF-κB pathway. Bortezomib is an inhibitor of proteasomes, which can induce apoptosis by inhibiting NF-κB pathway through suppressing degradation of IκBα. However, 3, 5-diethyl-1, 3, 5-thiadiazinane- 2-thione (DETT) can suppress IκBα phosphorylation and thus prevent IκBα from degradation by proteasomes [32]. During our study, the level of p-IκBα was significantly reduced by SZC015 (Fig. 6B), and therefore, we propose that inhibition of IκBα phosphorylation may be responsible for suppression of NF-κB signaling of SZC015-treated H322 cells. Phosphorylation of p65 at Ser536 site is considered to facilitate p65 nuclear translocation, which in turn modulates downstream gene expression [33]. Since p65 phosphorylation-dependent NF-κB activation plays critical roles in cancer cell survival [34]. Furthermore, we next evaluated the level of p65 and p-p65 in SZC015-treated H322 cells and found that the activity of both p65 and p-p65 in cytoplasm and p-p65 in nucleus, similar to bortezomib and DETT, were dramatically suppressed by our compound, indicating that nuclear translocation inhibition of p-p65 might be involved in suppression of NF-κB signaling. This conclusion was further confirmed by immunofluorescence staining of p65 (Fig. 6C). Taken together, the suppression of Akt/NF-κB signaling pathway is considered to be a very effective target for SZC015 in H322 cells.

Several natural compounds possess anticancer activity among many cancer types through autophagy-dependent mechanisms [35]. Autophagy is a process with “housekeeping” and “self-protective” functions under particular conditions. However, excessive autophagy could induce cell death and thus show anticancer activity in eukaryotic cells [36]. Many publications reported that OA induces cancer cells to undergo autophagy and thereby shows its anticancer function [37]. Interestingly, autophagy was strongly induced by SZC015, as compared with OA in H322 cells. Chloroquine is a late-stage inhibitor of autophagy [38]. Autophagy, which can be blocked by chloroquine [39], serves as an inducer of cancer cell death induced by SZC015 (Fig. 7). It is certainly complex between autophagy and apoptosis [25]. According to our results, autophagy induced by SZC015 served as an inhibitor of apoptosis

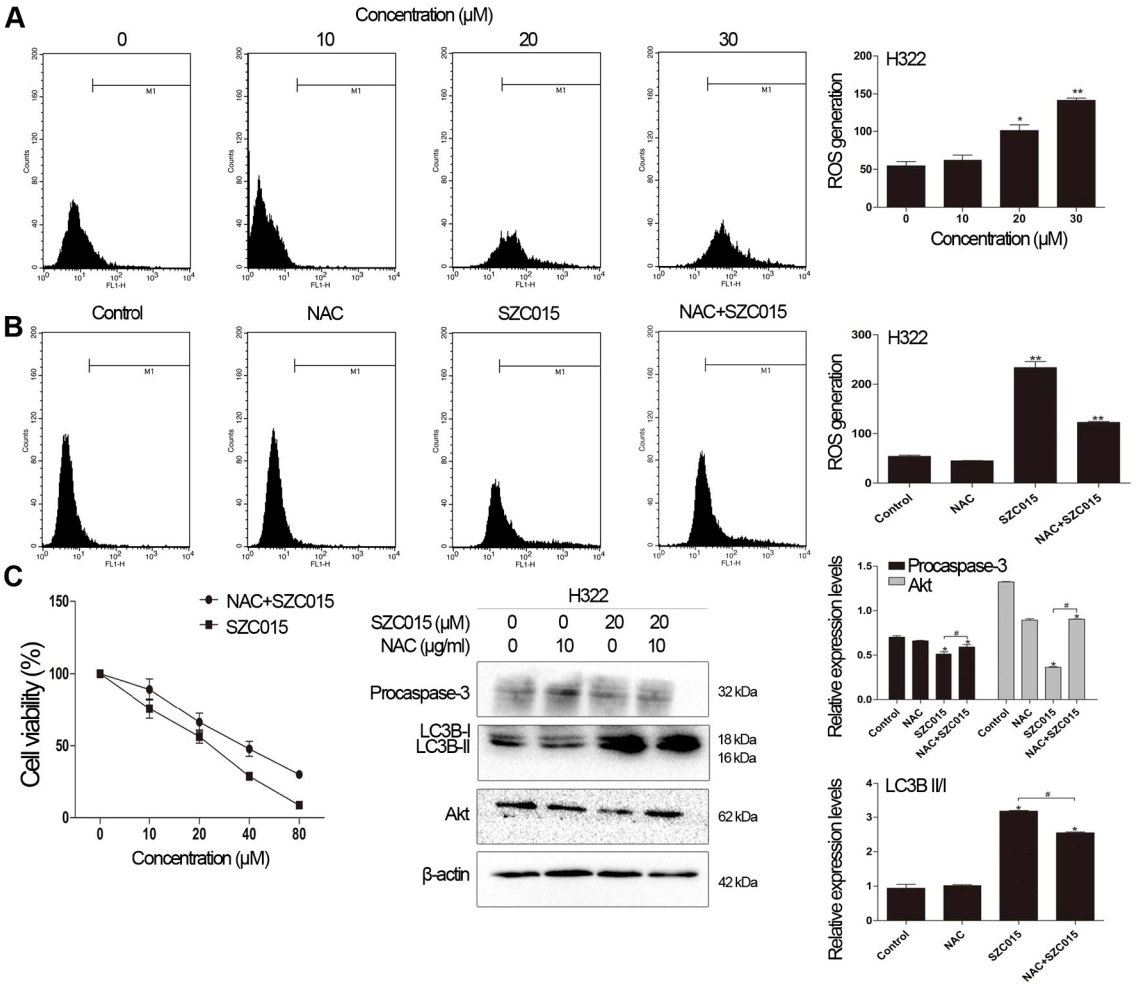

Fig. 8. Effect of SZC015 on intracellular ROS generation. **A.** SZC015 increased the intracellular ROS generation in H322 cells. Cells were treated with SZC015 at concentrations of 10, 20, and 30 μM for 24 h, and then the level of intracellular ROS was detected by flow cytometry. **B.** Effect of excessive ROS generation in SZC015-treated H322 cells. Cells were pretreated with 10 μg/ml NAC for 1 h and then treated with 20 μM SZC015 for more 24 h. **C.** Pretreatment with NAC (10 μg/ml) for 1 h increased the cell viability of SZC015-treated H322 cells. Western blot analysis of procaspase-3, LC3, and Akt, after pretreatment with 10 μg/ml NAC for 1 h. The data are shown as mean ± SD of three independent experiments. *Significantly different from control, $^{**}p < 0.01$, $^{*}p < 0.05$ and # significantly different from only SZC015 group, $\#p < 0.05$.

that triggered also by SZC015 in H322 cells (Fig. 7B). LC3B is the hallmark of the autophagy, the ratio of LC3II/I is increased after pre-treatment with CQ (Fig. 7B). In our study, apoptotic and autophagic cell death are two main death forms of SZC015 in H322 cells. ROS is considered to be an important upstream molecule involving in starvation-induced autophagy. Atg4 being inactivated by oxidative signal can promote the lipidation of Atg8 and thereby leads to autophagy [40]. Autophagy induction can be suppressed by NAC, suggesting that ROS is an upstream molecule of autophagy. NF-κB pathway also serves as a negative regulator of autophagy induced by ROS and starvation in many cell lines [41].

In summary, we demonstrated for the first time that SZC015 may be a potential anticancer compound against lung cancer cells in vitro. Our data also suggested that ROS is an upstream inhibitory modulator of Akt/NF-κB signaling and can trigger apoptosis and autophagy, which is a promoter of cell survival and an inhibitor of apoptosis in H322 cells. We concluded that SZC015 is a potent candidate agent for the prevention of cancer through apoptosis and autophagy-dependent mechanisms. However, more in vivo studies of SZC015 against other lung cancer cell lines and underlying mechanisms need to be further investigated.

Conflict of interest

The authors declare that they have no conflict of interest.

Acknowledgements

The present study was supported by the National Natural Science Foundation of China (no. 30772601) and the University Innovation Team Project Foundation of the Education Department of Liaoning (no. LT2013019).

References

[1] L.A. Torre, et al., Global cancer statistics, 2012, CA Cancer J. Clin. 65 (2) (2015) 87–108.
[2] To, C, et al., Dimethyl fumarate and the oleanane triterpenoids, CDDO-imidazolide and CDDO-methyl ester, both activate the Nrf2 pathway but have opposite effects in the A/J model of lung carcinogenesis, Carcinogenesis 36 (7) (2015) 769–781.
[3] M. Bartucci, et al., Therapeutic targeting of Chk1 in NSCLC stem cells during chemotherapy, Cell Death Differ. 19 (5) (2012) 768–778.
[4] J. Ma, et al., Pachymic acid induces apoptosis via activating ROS-dependent JNK and ER stress pathways in lung cancer cells, Cancer Cell Int. 15 (78) (2015) 015–0230.
[5] K.T. Liby, M.M. Yore, M.B. Sporn, Triterpenoids and rexinoids as multifunctional agents for the prevention and treatment of cancer, Nat. Rev. Cancer 7 (5) (2007) 357–369.
[6] K.T. Liby, M.B. Sporn, Synthetic oleanane triterpenoids: multifunctional drugs with a broad range of applications for prevention and treatment of chronic disease, Pharmacol. Rev. 64 (4) (2012) 972–1003.
[7] A.M. Sieuwerts, et al., The MTT tetrazolium salt assay scrutinized: how to use this assay reliably to measure metabolic activity of cell cultures in vitro for the assessment of growth characteristics, IC50-values and cell survival, Eur. J. Clin. Chem. Clin. Biochem. 33 (11) (1995) 813–823.
[8] C. Tolis, et al., Cell cycle disturbances and apoptosis induced by topotecan and gemcitabine on human lung cancer cell lines, Eur. J. Cancer 35 (5) (1999) 796–807.

[9] N. Mizushima, T. Yoshimori, B. Levine, Methods in mammalian autophagy research, Cell 140 (3) (2010) 313–326.
[10] Y.H. Ling, et al., PM02734 (elisidepsin) induces caspase-independent cell death associated with features of autophagy, inhibition of the Akt/mTOR signaling pathway, and activation of death-associated protein kinase, Clin. Cancer Res. 17 (16) (2011) 5353–5366.
[11] C. Li, et al., Molecular switch role of Akt in *Polygonatum odoratum* lectin-induced apoptosis and autophagy in human non-small cell lung cancer A549 cells, PLoS One (2014) 9(7).
[12] Y. Zhu, et al., *N*-acetyl cysteine protects human oral keratinocytes from Bis-GMA-induced apoptosis and cell cycle arrest by inhibiting reactive oxygen species-mediated mitochondrial dysfunction and the PI3K/Akt pathway, Toxicol. in Vitro 29 (8) (2015) 2089–2101.
[13] T.G. Cotter, Apoptosis and cancer: the genesis of a research field, Nat. Rev. Cancer 9 (7) (2009) 501–507.
[14] J.F. Kerr, A.H. Wyllie, A.R. Currie, Apoptosis: a basic biological phenomenon with wide-ranging implications in tissue kinetics, Br. J. Cancer 26 (4) (1972) 239–257.
[15] S. Ghosh, K. Bishayee, A.R. Khuda-Bukhsh, Oleanolic acid isolated from ethanolic extract of *Phytolacca decandra* induces apoptosis in A375 skin melanoma cells: drug-DNA interaction and signaling cascade, J Integr Med 12 (2) (2014) 102–114.
[16] H. Li, et al., Oleanolic acid inhibits proliferation and induces apoptosis in NB4 cells by targeting PML/RARalpha, Oncol. Lett. 6 (4) (2013) 885–890.
[17] V.V. Saralamma, et al., Poncirin induces apoptosis in AGS human gastric cancer cells through extrinsic apoptotic pathway by up-regulation of Fas ligand, Int. J. Mol. Sci. 16 (9) (2015) 22676–22691.
[18] S. Inoue, et al., CDDO induces apoptosis via the intrinsic pathway in lymphoid cells, Leukemia 18 (5) (2004) 948–952.
[19] S. Matsuyama, et al., Changes in intramitochondrial and cytosolic pH: early events that modulate caspase activation during apoptosis, Nat. Cell Biol. 2 (6) (2000) 318–325.
[20] X. Wang, et al., Inhibitory effect of oleanolic acid on hepatocellular carcinoma via ERK-p53-mediated cell cycle arrest and mitochondrial-dependent apoptosis, Carcinogenesis 34 (6) (2013) 1323–1330.
[21] C. Putinski, et al., Intrinsic-mediated caspase activation is essential for cardiomyocyte hypertrophy, Proc. Natl. Acad. Sci. U. S. A. 110 (43) (2013) 7.
[22] K.H. Seo, et al., Mangosenone F, a Furanoxanthone from *Garciana mangostana*, induces reactive oxygen species-mediated apoptosis in lung cancer cells and decreases xenograft tumor growth, Phytother. Res. 29 (11) (2015) 1753–1760.
[23] T. Efferth, et al., Artesunate induces ROS-mediated apoptosis in doxorubicin-resistant T leukemia cells, PLoS One (2007) 2(8).
[24] G. Chen, et al., An anti-leishmanial thiadiazine agent induces multiple myeloma cell apoptosis by suppressing the nuclear factor kappaB signalling pathway, Br. J. Cancer 110 (1) (2014) 63–70.
[25] L. Gao, et al., SZC017, a novel oleanolic acid derivative, induces apoptosis and autophagy in human breast cancer cells, Apoptosis 20 (12) (2015) 1636–1650.
[26] K.M. Holmstrom, T. Finkel, Cellular mechanisms and physiological consequences of redox-dependent signalling, Nat Rev Mol Cell Biol 15 (6) (2014) 411–421.
[27] S. Liu, et al., NF-kappaB activation was involved in reactive oxygen species-mediated apoptosis and autophagy in 1-oxoeudesm-11(13)-eno-12,8alpha-lactone-treated human lung cancer cells, Arch. Pharm. Res. 37 (8) (2014) 1039–1052.
[28] Y.C. Li, et al., Plumbagin induces apoptotic and autophagic cell death through inhibition of the PI3K/Akt/mTOR pathway in human non-small cell lung cancer cells, Cancer Lett. 344 (2) (2014) 239–259.
[29] T.D. Gilmore, M. Herscovitch, Inhibitors of NF-kappaB signaling: 785 and counting, Oncogene 25 (51) (2006) 6887–6899.
[30] H.J. Kim, N. Hawke, A.S. Baldwin, NF-kappaB and IKK as therapeutic targets in cancer, Cell Death Differ. 13 (5) (2006) 738–747.
[31] C.H. Lee, et al., NF-kappaB as a potential molecular target for cancer therapy, Biofactors 29 (1) (2007) 19–35.
[32] C.Y. Sasaki, et al., Phosphorylation of RelA/p65 on serine 536 defines an I{kappa}B{alpha}-independent NF-{kappa}B pathway, J. Biol. Chem. 280 (41) (2005) 34538–34547.
[33] D.K. Lee, et al., FBI-1 enhances transcription of the nuclear factor-kappaB (NF-kappaB)-responsive E-selectin gene by nuclear localization of the p65 subunit of NF-kappaB, J. Biol. Chem. 280 (30) (2005) 27783–27791.
[34] C. Kaewpiboon, et al., Feroniellin A-induced autophagy causes apoptosis in multidrug-resistant human A549 lung cancer cells, Int. J. Oncol. 44 (4) (2014) 1233–1242.
[35] L. Yu, M.J. Lenardo, E.H. Baehrecke, Autophagy and caspases: a new cell death program, Cell Cycle 3 (9) (2004) 1124–1126.
[36] L.X. Rui, et al., The dual induction of apoptosis and autophagy by SZC014, a synthetic oleanolic acid derivative, in gastric cancer cells via NF-kappaB pathway, Tumour Biol. 7 (2015) 7.
[37] J. Liu, et al., Oleanolic acid induces protective autophagy in cancer cells through the JNK and mTOR pathways, Oncol. Rep. 32 (2) (2014) 567–572.
[38] T. Kimura, et al., Chloroquine in cancer therapy: a double-edged sword of autophagy, Cancer Res. 73 (1) (2013) 3–7.
[39] H. Maes, et al., Tumor vessel normalization by chloroquine independent of autophagy, Cancer Cell 26 (2) (2014) 190–206.
[40] R. Scherz-Shouval, et al., Reactive oxygen species are essential for autophagy and specifically regulate the activity of Atg4, EMBO J. 26 (7) (2007) 1749–1760.
[41] M. Djavaheri-Mergny, et al., NF-kappaB activation represses tumor necrosis factor-alpha-induced autophagy, J. Biol. Chem. 281 (41) (2006) 30373–30382.